

A Third Mode of DNA Binding: Phosphate Clamps by a Polynuclear Platinum Complex

Seiji Komeda,^{†,‡,§} Tinoush Moulaei,[†] Kristen Kruger Woods,[†] Masahiko Chikuma,[‡]
Nicholas P. Farrell,^{*,§} and Loren Dean Williams^{*,†,||}

Contribution from the School of Chemistry and Biochemistry, Georgia Institute of Technology, Atlanta, Georgia 30332-0400, Osaka University of Pharmaceutical Sciences, Takatsuki, 569-1094, Japan, Department of Chemistry, Virginia Commonwealth University, Richmond, Virginia 23284-2006, and Department of Chemistry, Western Washington University, Bellingham, Washington 98225-9150

Received April 24, 2006; E-mail: npfarrell@vcu.edu; loren.williams@chemistry.gatech.edu

Abstract: We describe a 1.2 Å X-ray structure of a double-stranded B-DNA dodecamer (the Dickerson Dodecamer, DDD, [d(CGCGAATTCGCG)]₂) associated with a cytotoxic platinum(II) complex, [*trans*-Pt(NH₃)₂(NH₂(CH₂)₆(NH₃⁺))₂]-μ-*trans*-Pt(NH₃)₂(NH₂(CH₂)₆NH₂)₂] (TriplatinNC). TriplatinNC is a multifunctional DNA ligand, with three cationic Pt(II) centers, and directional hydrogen bonding functionalities, linked by flexible hydrophobic segments, but without the potential for covalent interaction. TriplatinNC does not intercalate nor does it bind in either groove. Instead, it binds to phosphate oxygen atoms and thus associates with the backbone. The three square-planar tetra-am(m)ine Pt(II) coordination units form bidentate N→O→N complexes with OP atoms, in a motif we call the Phosphate Clamp. The geometry is conserved among the 8 observed phosphate clamps in this structure. The interaction appears to prefer O2P over O1P atoms (frequency of interaction is O2P > O1P, base and sugar oxygens > N). The high repetition and geometric regularity of the motif suggests that this type of Pt(II) center can be developed as a modular nucleic acid binding device with general utility. TriplatinNC extends along the phosphate backbone, in a mode of binding we call “Backbone Tracking” and spans the minor groove in a mode of binding we call “Groove Spanning”. Electrostatic forces appear to induce modest DNA bending into the major groove. This bending may be related to the direct coordination of a sodium cation by a DNA base, with unprecedented inner-shell (direct) coordination of penta-hydrated sodium at the O6 atom of a guanine.

Introduction

Intercalation of planar molecules into DNA, proposed by Lerman in 1961,^{1,2} is a broadly employed binding mode for natural and synthetic DNA ligands. Minor groove association of arc-shaped molecules, proposed by Wells in 1974,³ has been validated as a second key binding mode. Essentially all previously described noncovalent DNA ligands can be broadly broken down into intercalators (such as proflavin), groove binders (such as distamycin), or multifunctional groove-binding intercalators (such as daunomycin), reviewed by Wilson.⁴

This report describes what appears to be a discrete *third* mode of binding, with interactions that exclusively utilize backbone functional groups. The backbone-binding mode falls cleanly outside the previous groove-binder and intercalator classes.

Backbone-binding is accomplished here with multinuclear Pt(II) compounds. Pt(II) centers can be assembled with various linkers and diverse spacings, orientations and reactivities of the Pt(II) centers to form a variety of DNA and RNA ligands. TriplatinNC ([*trans*-Pt(NH₃)₂(NH₂(CH₂)₆(NH₃⁺))₂]-μ-*trans*-Pt(NH₃)₂(NH₂(CH₂)₆NH₂)₂](NO₃)₈), the trinuclear Pt(II) compound cocrystallized with DNA for this study, is shown in Figure 1A.

A drug-design effort by Farrell and co-workers has led to development of both reactive ligands,^{5,6} which form covalent adducts to DNA, and nonreactive ligands,^{7,8} which bind exclusively by noncovalent interactions. BBR3464 (Figure 1C) is capable of bifunctional covalent binding to DNA in a manner distinct from mononuclear species such as cisplatin (see below). To obtain noncovalent compounds, substitution-labile chlorides of reactive Pt(II) compounds can be replaced with inert ammine or amine ligands,^{7,8} which do not form Pt–DNA bonds but

[†] Georgia Institute of Technology.

[‡] Osaka University of Pharmaceutical Sciences.

[§] Virginia Commonwealth University.

^{||} Western Washington University.

(1) Lerman, L. S. *J. Mol. Biol.* **1961**, *3*, 18–30.
(2) Lerman, L. S. *J. Cell Comput. Physiol.* **1964**, *64* (suppl. 1), 1–18.
(3) Wartell, R. M.; Larson, J. E.; Wells, R. D. *J. Biol. Chem.* **1974**, *249*, 6719–31.
(4) Wilson, W. D. Reversible Interactions of Small Molecules with Nucleic Acids. In *Nucleic Acids in Chemistry and Biology*; IRL Press at Oxford University Press: Oxford, 1990.

(5) Manzotti, C.; Pratesi, G.; Menta, E.; Di Domenico, R.; Cavalletti, E.; Fiebig, H. H.; Kelland, L. R.; Farrell, N.; Polizzi, D.; Supino, R.; Pezzoni, G.; Zunino, F. *Clin. Cancer Res.* **2000**, *6*, 2626–34.
(6) Farrell, N. *Met. Ions Biol. Sys.* **2004**, *41*, 252–96.
(7) Qu, Y.; Harris, A.; Hegmans, A.; Petz, A.; Kabolizadeh, P.; Penazova, H.; Farrell, N. *J. Inorg. Biochem.* **2004**, *98*, 1591–8.
(8) Harris, A.; Qu, Y.; Farrell, N. *Inorg. Chem.* **2005**, *44*, 1196–8.

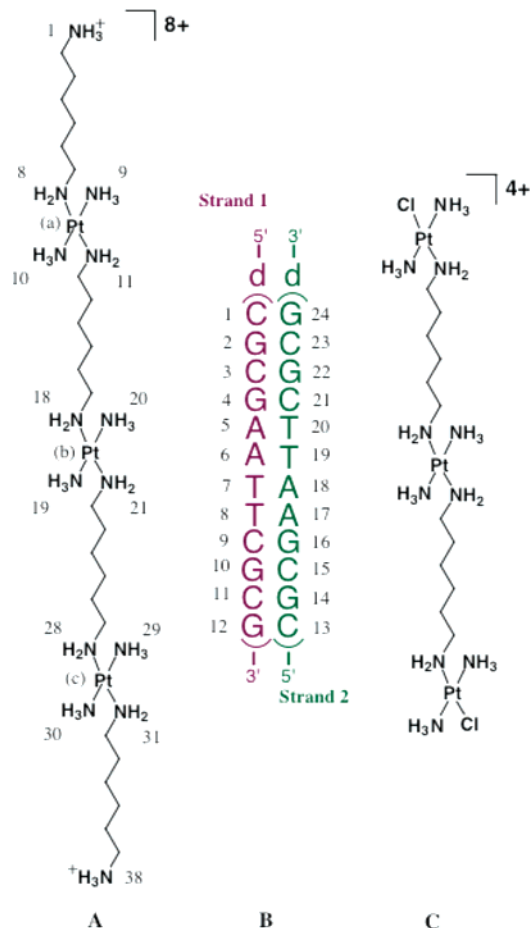


Figure 1. (A) Chemical structure of the trinuclear platinum(II) compound, TriplatinNC [$\{trans\text{-Pt}(\text{NH}_3)_2(\text{NH}_2(\text{CH}_2)_6(\text{NH}_3^+))\}_2\text{-}\mu\text{-}\{trans\text{-Pt}(\text{NH}_3)_2(\text{NH}_2(\text{CH}_2)_6\text{NH}_2)_2\}$] $^{8+}$, which was cocrystallized with DNA. (B) Double-stranded dodecamer duplex, $[\text{d}(\text{CGCGAATTCGCG})]_2$ (DDD), used for this crystallographic study. (C) For comparison, a cross-linking trinuclear platinum(II) complex, $[\{trans\text{-Pt}(\text{NH}_3)_2\text{Cl}\}_2\text{-}\mu\text{-}\{trans\text{-Pt}(\text{NH}_3)_2(\text{NH}_2(\text{CH}_2)_6\text{NH}_2)_2\}]^{4+}$ (BBR3464), with labile chloride ligands.

which retain high DNA affinity. TriplatinNC is a noncovalent ligand, with stable “dangling” hexanediamine ligands substituted for the reactive chloride ligands.

Here we describe the three-dimensional structure of TriplatinNC bound to the Dickerson-Drew Dodecamer (DDD),⁹ which is the self-complementary double-stranded DNA fragment $[\text{d}(\text{CGCGAATTCGCG})]_2$ (Figure 1B). The structure of this DNA complex at 1.2 Å resolution shows that TriplatinNC has unprecedented selectivity for phosphate oxygens, forming bidentate $\text{NH}\cdots\text{O}\cdots\text{HN}$ (amine \cdots phosphate \cdots ammine) complexes through hydrogen-bonding interactions. The high frequency and geometric regularity of these “Phosphate Clamps” in the DDD–TriplatinNC complex suggest that Pt(II) units can be utilized as generalizable nucleic acid binding elements. These elements might be assembled by either design or selection, to target any structured nucleic acid, including ribosomes. An additional unique feature of this complex, indicated by a comparison with the results of a 2003 survey of the structural database¹⁰ and a more recent survey (S.K., unpublished), include

direct coordination of sodium at O6 of a guanine, in the major groove of B-form DNA. The ensuing charge neutralization appears to induce modest DNA bending.

Our work here builds on the discovery and development of the clinical anticancer drug, cisplatin (*cis*-diamminedichloro-platinum(II)),^{11,12} which provided the first evidence that Pt(II)–DNA interactions could be of great importance in drug action. Cisplatin forms covalent DNA adducts such as 1,2-intrastrand cross-links, which result in severe DNA distortions.^{13–16} The conformations of the DNA adducts are thought to be critical parameters in the mechanism of cisplatin cytotoxicity and antitumor activity. Cisplatin induces cellular resistance, which is in part manifested through tolerance and enhanced repair of DNA lesions.^{17,18} Most mononuclear cisplatin analogues, such as carboplatin [*cis*-diammine(1,1-cyclobutancarboxylato))-platinum(II)] show cross-resistance to cisplatin.¹⁹

Long-range {Pt,Pt} cross-links of polyamine-bridged di- and trinuclear Pt(II) complexes were predicted to induce DNA distortions that are structurally distinct from those induced by the short-range cisplatin cross-links.^{6,20–24} It was hypothesized that DNA adducts that are distinct from those of cisplatin could circumvent clinical resistance to the parent drug.²⁵ The prototypic drug resulting from this design philosophy, BBR3464, exhibits high potency against cisplatin-resistant tumor cells, and has undergone Phase II clinical trials.⁶ Preassociation with DNA is an important mechanistic feature of BBR3464 and may be significant in efficiency and specificity of cross-link formation. Study of noncovalent ligands allows the effects of preassociation to be examined in the absence of covalent cross-linking. This paper describes the likely preassociation mode of BBR3464 with DNA.

Methods

Crystallization. The ammonium salt of reverse-phase HPLC-purified $\text{d}(\text{CGCGAATTCGCG})$ (Integrated DNA Technologies, Coralville, IA) was combined with TriplatinNC, synthesized by the method previously reported.⁷ Crystals were grown in hanging drops by vapor diffusion from a solution initially containing 0.19 mM $[\text{d}(\text{CGCGAATTCGCG})]_2$, 0.19 mM TriplatinNC, 31 mM sodium cacodylate, pH 6.5, 9.6 mM magnesium chloride, and 6.9% 2-methyl-2,4-pentenediol (MPD). The crystallization solution was equilibrated against a reservoir of 30% MPD at 20 °C in a constant-temperature incubator. Orthorhombic ($P2_12_12_1$) crystals appeared within several days. The crystal chosen for data collection was $0.2 \times 0.2 \times 0.2 \text{ mm}^3$.

(9) Wing, R.; Drew, H.; Takano, T.; Broka, C.; Takana, S.; Itakura, K.; Dickerson, R. E. *Nature* **1980**, *287*, 755–8.

(10) Howerton, S. B.; Nagpal, A.; Williams, L. D. *Biopolymers* **2003**, *69*, 87–99.

(11) Rosenberg, B.; Vancamp, L.; Trosko, J. E.; Mansour, V. H. *Nature* **1969**, *222*, 385–6.

(12) Rosenberg, B.; Vancamp, L.; Krigas, T. *Nature* **1965**, *205*, 698–9.

(13) Jamieson, E. R.; Lippard, S. J. *Chem. Rev.* **1999**, *99*, 2467–98.

(14) Takahara, P. M.; Rosenzweig, A. C.; Frederick, C. A.; Lippard, S. J. *Nature* **1995**, *377*, 649–52.

(15) Brabec, V.; Kleinwachter, V.; Butour, J. L.; Johnson, N. P. *Biophys. Chem.* **1990**, *35*, 129–41.

(16) van Boom, S. S. G. E.; Yang, D. Z.; Reedijk, J.; van der Marel, G. A.; Wang, A. H. J. *J. Biomol. Struct. Dyn.* **1996**, *13*, 989–98.

(17) Andrews, P. A.; Murphy, M. P.; Howell, S. B. *Eur. J. Cancer Clin. Oncol.* **1989**, *25*, 619–25.

(18) Tashiro, T. *Gan To Kagaku Ryoho* **1990**, *17*, 509–14.

(19) Gore, M. E.; Fryatt, I.; Wiltshaw, E.; Dawson, T.; Robinson, B. A.; Calvert, A. H. *Br. J. Cancer* **1989**, *60*, 767–9.

(20) Hegmans, A.; Berners-Price, S. J.; Davies, M. S.; Thomas, D. S.; Humphreys, A. S.; Farrell, N. *J. Am. Chem. Soc.* **2004**, *126*, 2166–80.

(21) Farrell, N.; Qu, Y.; Feng, L.; Vanhouten, B. *Biochemistry* **1990**, *29*, 9522–31.

(22) Zou, Y.; Vanhouten, B.; Farrell, N. *Biochemistry* **1993**, *32*, 9632–8.

(23) Cox, J. W.; Berners-Price, S.; Davies, M. S.; Qu, Y.; Farrell, N. *J. Am. Chem. Soc.* **2001**, *123*, 1316–26.

(24) Qu, Y.; Scarsdale, N. J.; Tran, M. C.; Farrell, N. P. *J. Biol. Inorg. Chem.* **2003**, *8*, 19–28.

(25) Farrell, N. *Cancer Invest.* **1993**, *11*, 578–89.

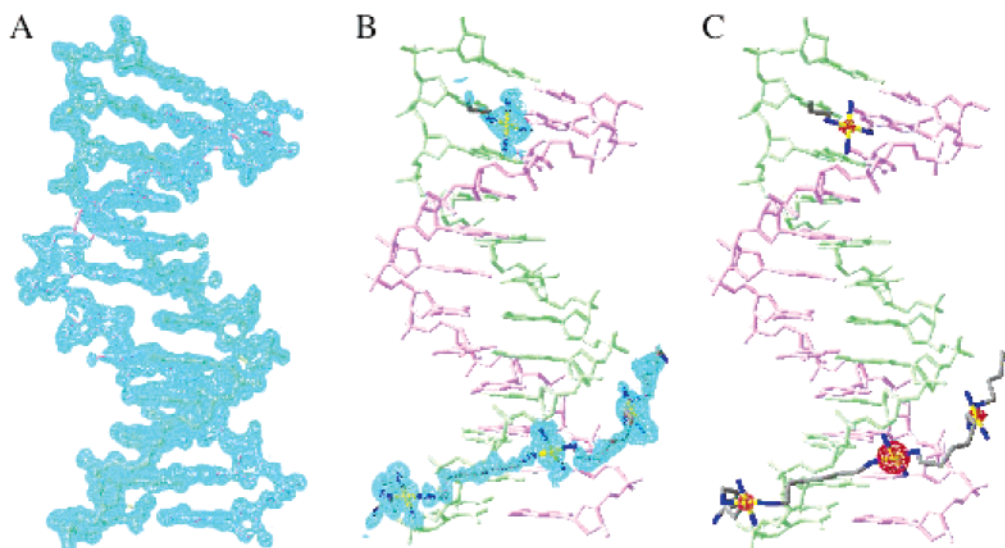


Figure 2. Electron density maps of the TriplatinNC–DNA complex. Both TriplatinNC^a and TriplatinNC^b are shown. (A) Sum electron density surrounding the DNA, contoured at 1.5σ . TriplatinNC^a and TriplatinNC^b are omitted for clarity. (B) Sum $(2F_o - F_c)$ electron density surrounding TriplatinNC^a and TriplatinNC^b, contoured at 0.9σ . (C) Anomalous electron density contoured at 5σ . The positions of the Pt(II) atoms are indicated by the anomalous peaks.

Table 1. Data Collection and Refinement Statistics

unit cell dimensions	$\alpha = \beta = \gamma = 90^\circ$ $a = 23.675 \text{ \AA}, b = 41.692 \text{ \AA}, c = 65.651 \text{ \AA}$
DNA (asymmetric unit)	[d(CGCGAATTCGCG)] ₂
space group	$P2_12_12_1$
temperature of data collection (K)	175
number of unique reflections	21 375
number of reflections used in refinement ($F > 2\sigma F$)	18 995
RMS deviation of bonds from ideality (\AA)	0.012
RMS deviation of angles from ideality (\AA)	0.022
max. resolution of observed reflections (\AA)	1.07
max. resolution of refinement (\AA)	1.13
number of DNA atoms	486
number of TriplatinNC atoms	49
number of water molecules, excluding sodium first shell	120
number of sodium ions plus coordinating water molecules	6
R -factor (% , $F > 2\sigma F$)	18.18
R -free (% , all)	23.21

Data Collection. Diffraction data were collected on beamline X26C at the National Synchrotron Light Source, Brookhaven National Laboratory. Frames (360) of intensity data (oscillation angle = 1.0°) were collected at 175 K at a wavelength of 1.05 \AA and recorded on an ADSC-Quantum 4 CCD detector. Data were merged and reduced with HKL2000.²⁶ Data collection and reduction statistics are given in Table 1.

Structure Solution and Refinement. A starting DNA model consisted of coordinates of [d(CGCGAATTCGCG)]₂ (NDB²⁷ entry bdl084²⁸) excluding solvent and ions. After a rotation/translation search and rigid body refinement with CNS version 1.1,²⁹ the R -factor/ R -free were 43/44%. Strong sum and difference peaks indicated positions of three Pt²⁺ atoms, which were added to the model, giving R -factor/ R -free of 31/32%. The R -factor/ R -free dropped to 21/23% upon addition of 96 water molecules along with additional atoms of TriplatinNC. A

fragment of a second TriplatinNC molecule, which is partially disordered, was added to the model, contributing only one platinum coordination sphere and a portion of aliphatic chain. The initial TriplatinNC models were generated using ChemBats3D Pro version 4.0 (CambridgeSoft).

The four Pt²⁺ positions were confirmed by anomalous maps, which were computed using phases of only a single Pt²⁺ atom, with the program CNS. During the refinement a peak of electron density surrounded by a well-formed octahedron of atoms was assigned as a sodium ion. This assignment is based on ligand to Na⁺ distances of around 2.4 \AA . In the final model, the maps are clean and continuous around the DNA, and the assigned TriplatinNC atoms (Figure 2).

The occupancies of the TriplatinNC molecules were estimated using the Pt²⁺ atoms. Occupancies were optimized throughout the refinement by fitting statistics and by examination of $\pm(F_o - F_c)$ maps. Thirty cycles of refinement were carried out using the program SHELXL 97,³⁰ during which anisotropic thermal factor refinement was performed for the DNA atoms and the Na⁺ ion plus its first hydration shell. Other solvent (water) and TriplatinNC molecules were treated isotropically. A loose distance restraint of Na⁺ – O (O6 of G22 or water oxygen) to sodium was maintained at 2.40 \AA .³¹ Restraints were not applied to O–Na⁺–O angles. The refinement converged to a final R -factor/ R -free of 18/23%. Helical parameters were calculated using a program, CURVES 5.3.^{32,33} Structure refinement statistics are given in Table 1.

(30) Sheldrick, G. M. *SHELX-97*; Gottingen University: Germany, 1997.

(26) Otwinowski, Z.; Minor, W. Processing of X-ray Diffraction Data Collected in Oscillation Mode. In *Methods Enzymology, Macromolecular Crystallography*; Carter, J. C. W., Sweet, R. M., Eds.; Academic Press: New York, 1997; Vol. 276, Part A, pp 307–26.

(27) Berman, H. M.; Olson, W. K.; Beveridge, D. L.; Westbrook, J.; Gelbin, A.; Demeny, T.; Hsieh, S.-H.; Srinivasan, A. R.; Schneider, B. *Biophys. J.* **1992**, *63*, 751–9.

(28) Shui, X.; McFail-Isom, L.; Hu, G. G.; Williams, L. D. *Biochemistry* **1998**, *37*, 8341–55.

(29) Brunger, A. T.; Adams, P. D.; Clore, G. M.; DeLano, W. L.; Gros, P.; Grosse-Kunstleve, R. W.; Jiang, J. S.; Kuszewski, J.; Nilges, M.; Pannu, N. S.; Read, R. J.; Rice, L. M.; Simonson, T.; Warren, G. L. *Acta Crystallogr., Sect. D: Biol. Crystallogr.* **1998**, *54*, 905–21.

Platinum positions were initially established from intense peaks in sum ($2F_o - F_c$) maps, and were confirmed by anomalous peaks ($F_+ - F_-$, Figure 2C). The anomalous electron density is consistent with the Pt(II) positions initially determined from sum electron density map.

TriplatinNC–DNA Interactions. Backbone Tracking and Groove Spanning. The DDD–TriplatinNC crystal appears to be stabilized by an extensive hydrogen bonding and electrostatic network between the DNA and TriplatinNC. A schematic representation of the hydrogen bonding interactions is shown in Figure 3. A plurality of the TriplatinNC^a–DNA hydrogen bonds (six hydrogen bonds) are with one strand of DNA (Figures 3 and 4). We refer to this mode of backbone binding as “Backbone Tracking”. TriplatinNC^a also forms four hydrogen bonds with a second duplex. In this case, TriplatinNC^a interacts with two phosphate groups that are juxtaposed across the minor groove (Figures 3 and 5, sym 1). We refer to this mode of backbone binding as “Groove Spanning”. As described in detail below, Backbone Tracking and Groove Spanning employ the same fundamental binding motif. The two modes may coexist in solution.

Oxygen Selectivity. TriplatinNC shows selectivity for DNA oxygens and selectivity against DNA nitrogen atoms (Figure 3). TriplatinNC^a and TriplatinNC^b, in combination, form 27 hydrogen bonds with DNA. Twenty six of those hydrogen bonds are with oxygen atoms. Only a single hydrogen bond links TriplatinNC to a nitrogen atom (N7 of G, sym 4) in this structure. In addition TriplatinNC shows selectivity for phosphate oxygen atoms over other oxygen atoms. Twenty one of the 26 TriplatinNC–oxygen hydrogen bonds are with phosphate oxygens. To our knowledge, TriplatinNC is the first phosphate-selective DNA ligand observed. Only four TriplatinNC hydrogen bonds involve O6 positions of guanines. One TriplatinNC hydrogen bond is with a terminal hydroxyl group.

The Phosphate Clamp. In the structure described here, the square-planar tetra-am(m)ine Pt(II) coordination unit forms bidentate complexes with OP atoms (Figures 4–7). Binding, with high selectivity and specific geometry, involves two *cis*-am(m)ine ligands of a given Pt(II), an arrangement that is called here the *Phosphate Clamp*. A Phosphate Clamp is a cyclic structure with a single OP, which accepts two hydrogen bonds, one from each of two am(m)ine ligands of a single Pt(II) center (Figures 6 and 7). As indicated in Table 2, the geometry of the motif (Figure 7D) is highly conserved. The maximum number of Phosphate Clamps observed here with a single tetra-am(m)ine Pt(II) coordination unit is three (Figure 6). A Phosphate Clamp appears to require *cis*-orientation of the am(m)ine ligands of Pt(II). Mutually *trans*-am(m)ine ligands do not participate in Phosphate Clamps because the distance between hydrogen bond donors is too large and their orientations are in opposing directions.

The four observed tetra-am(m)ine Pt(II) coordination units of TriplatinNC^a and TriplatinNC^b contain 16 potential Phosphate Clamps, of which eight are utilized. Each tetra-am(m)ine Pt(II) coordination unit engages in at least one Phosphate Clamp (Figure 7C). Using this motif, the three Pt(II) centers of TriplatinNC^a bind seven OP atoms. Pt(a) engages three phosphate oxygens (Figure 6) in Phosphate Clamps. Pt(b) engages two phosphate oxygens. Pt(c) engages two phosphate oxygens, and binds by an alternative mode in which one ammine group

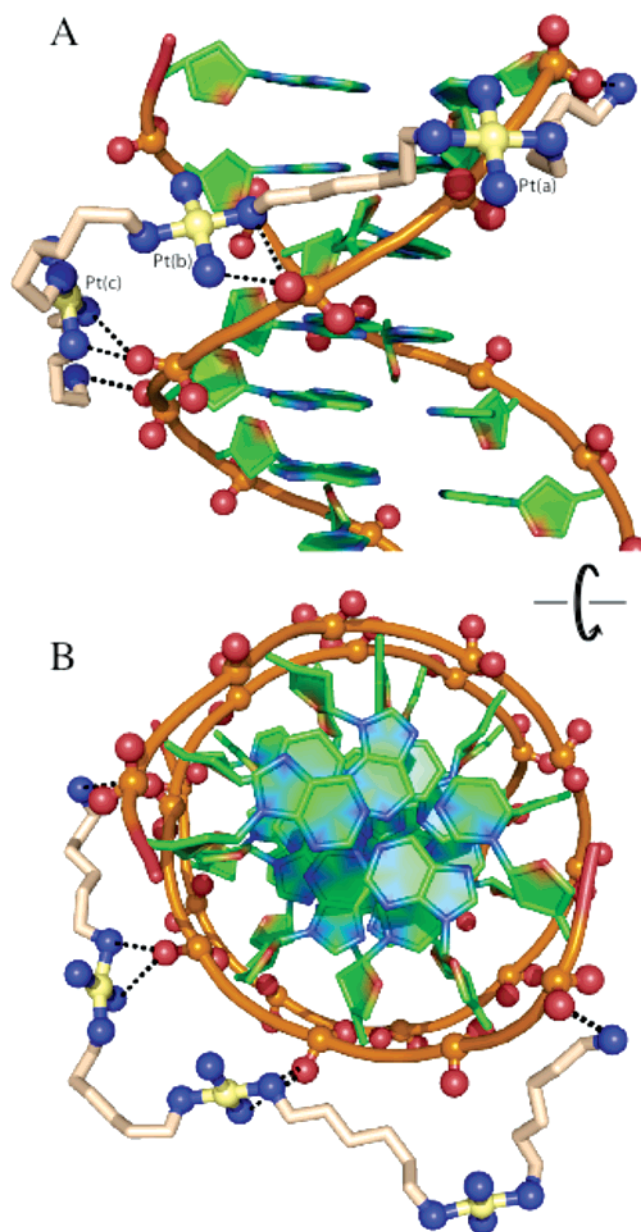


Figure 4. Backbone Tracking. Hydrogen bonds between TriplatinNC^a and DNA are indicated by dashed lines. Two Phosphate Clamps are shown. Both dangling amines form hydrogen bonds with phosphate groups. (A) View perpendicular to the helical axis. (B) View along the helical axis. Atoms are colored by type with carbon (DNA), green; carbon (TriplatinNC) gray; nitrogen, blue; oxygen, red; platinum, yellow. The phosphodiester backbone of the DNA is represented by a tube. The P, O1P, and O2P atoms and are ball-and-stick. TriplatinNC is represented by stick, except for the nitrogen and platinum atoms, which are ball-and-stick. This and some of the other Figures in this manuscript were made in part with Pymol (Warren L. DeLano “The PyMOL Molecular Graphics System.” DeLano Scientific LLC, San Carlos, CA, USA <http://www.pymol.org>).

interacts with both O1P and O2P of a single phosphate group. The single observed Pt(II) center of TriplatinNC^b binds one phosphate oxygen in a Phosphate Clamp (Figure 3).

It appears that Phosphate Clamps form preferentially with O2P atoms over O1P atoms as seven of eight observed Phosphate Clamps involve O2P atoms. This preference may be dependent on the conformation and state of the nucleic acid. The O2P/O1P selectivity in A-form RNA or in other nucleic acid forms may differ from that in B-form DNA.

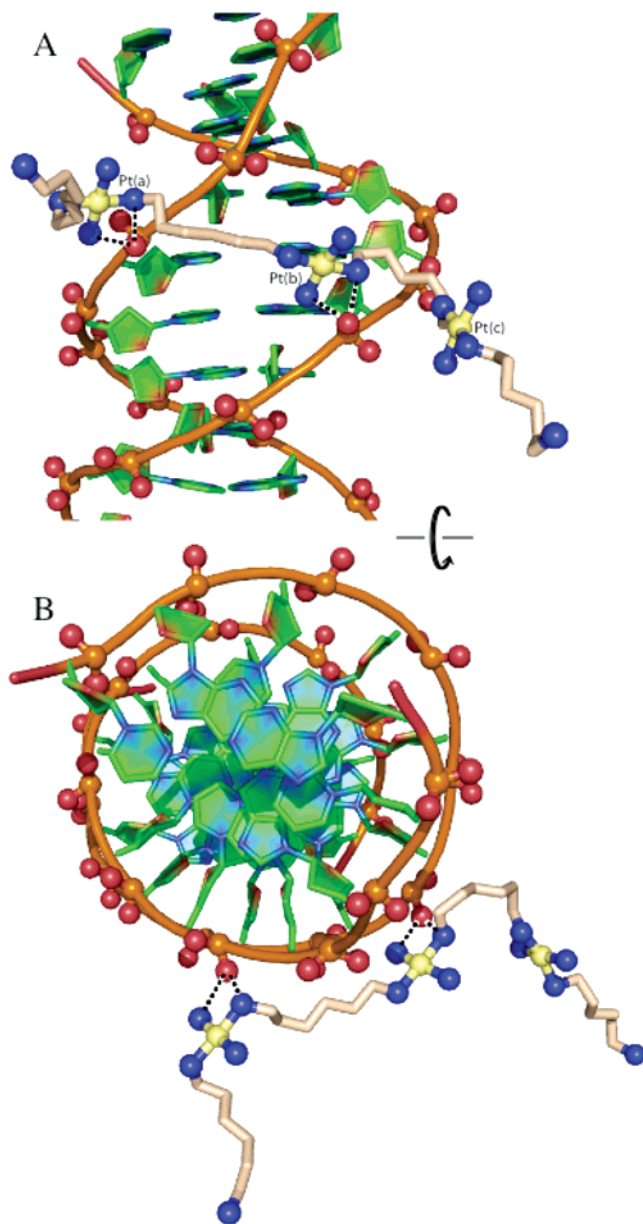


Figure 5. Groove Spanning. Hydrogen bonds between TriplatinNC^a and DNA (sym 1) are indicated by dashed lines. There are two Phosphate Clamps, with which TriplatinNC^a bridges two strands across the minor groove of a DNA duplex, at the lip of the minor-groove, defined in Sines et al.³⁴ (A) View perpendicular to the helical axis. (B) View along the helical axis. Atoms are colored and coded as in Figure 4.

Dangling Amines. The terminal amino groups of TriplatinNC^a form hydrogen bonds to the same DNA strand (Figures 3 and 4). Each of the terminal amino groups (N1 and N38) of TriplatinNC^a forms a hydrogen bond with a phosphate oxygen (G14 and A18, respectively).

Backbone Tracking versus Groove Spanning. Preferential interaction with phosphate oxygens causes TriplatinNC^a to track the backbone, linking adjacent phosphate groups of DNA (Figures 3 and 4, sym 0). TriplatinNC^a interacts with four out of five consecutive phosphate groups as it tracks the backbone. Six hydrogen bonds stabilize this backbone tracking complex.

In addition, Pt(a) and Pt(b) form phosphate clamps on opposite sides of the minor groove (Figures 3 and 5, sym 1). In this way, TriplatinNC^a bridges two paired strands, and spans the minor groove. Opposing edges of the minor groove are

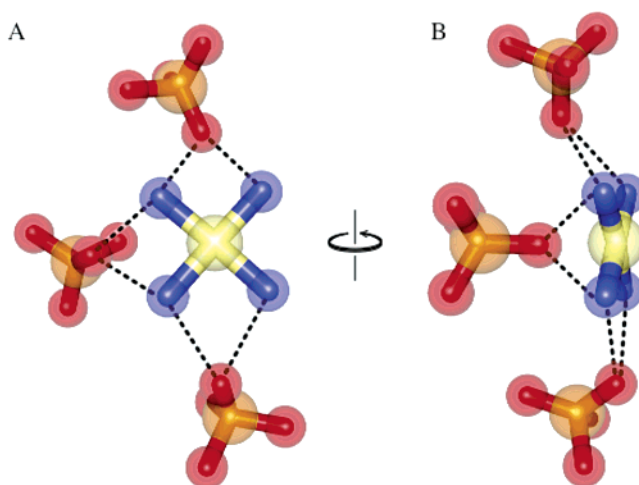


Figure 6. Multiple Phosphate Clamps formed by a single Pt(II) center. The am(m)ine groups of Pt(a) form hydrogen bonds with O2P atoms of three DNA duplexes (Sym 2, Sym 3, and Sym 4, Figure 3). (A) View along the normal of the Pt(II) center. (B) View roughly along the perpendicular of the Pt(II) center. The atoms are colored as in Figure 4. For clarity, only one tetra-am(m)ine Pt(II) center of TriplatinNC^a (Pt(a)) and the relevant phosphate atoms (O2P, O2P, O5', O3', and P) are shown.

linked by clamps of Pt(a) with the O2P of T(7) and of Pt(b) to the O2P of C(21). TriplatinNC^a is located in part at the lip of the minor-groove as defined in Sines et al.³⁴ Four hydrogen bonds stabilize the groove-spanning binding mode of TriplatinNC^a.

In solution TriplatinNC may bind by a mixture of “backbone tracking” and “groove spanning” modes, with both utilizing Phosphate Clamps. Note that minor groove binders bind to the central region of the DDD because they interact directly with A and T bases, on their minor groove edges. For phosphate clamps, no such selectivity for the central region is anticipated, nor is it observed.

Lattice Interactions. TriplatinNC engages in a complex network of lattice interactions (Figures 3 and 6C). However, the mode of interaction, in particular the Phosphate Clamp, is highly conserved throughout this network. This conservation of interaction mode suggests that it would similarly be manifest on isolated DNA molecules in solution, although possibly at lower frequency. TriplatinNC^a interacts with a total of six symmetry-related DDD duplexes. These lattice interactions, with the exception of one set of TriplatinNC^a–guanine interactions (above), are all with DNA phosphate oxygens (Figure 3). TriplatinNC^b interacts with three duplexes. TriplatinNC^b bridges three different symmetry related duplexes, two of them at their termini. TriplatinNC, like multivalent inorganic cations and polyamines, should stabilize DNA, and under appropriate conditions, condense DNA.^{35,36}

Innershell Coordination of a Sodium Ion by the O6 of a Guanine. In the DDD–TriplatinNC complex described here, a Na⁺ ion is located in the major groove (Figures 3 and 8). The Na⁺ ion is partially dehydrated and interacts directly with the edge of a guanine. Innershell coordination of a Na⁺ to the O6

(34) Sines, C. C.; McFail-Isom, L.; Howerton, S. B.; VanDerveer, D.; Williams, L. D. *J. Am. Chem. Soc.* **2000**, *122*, 11048–56.

(35) Anderson, C. F.; Record, M. T., Jr. *Annu. Rev. Phys. Chem.* **1995**, *46*, 657–700.

(36) Bloomfield, V. A.; Wilson, R. W. Interactions of Polyamines with Polynucleotides. In *Polyamines in Biology and Medicine*; Morris, D. R., Marton, L. J., Eds.; Marcel Dekker: New York, 1981; pp 183–206.

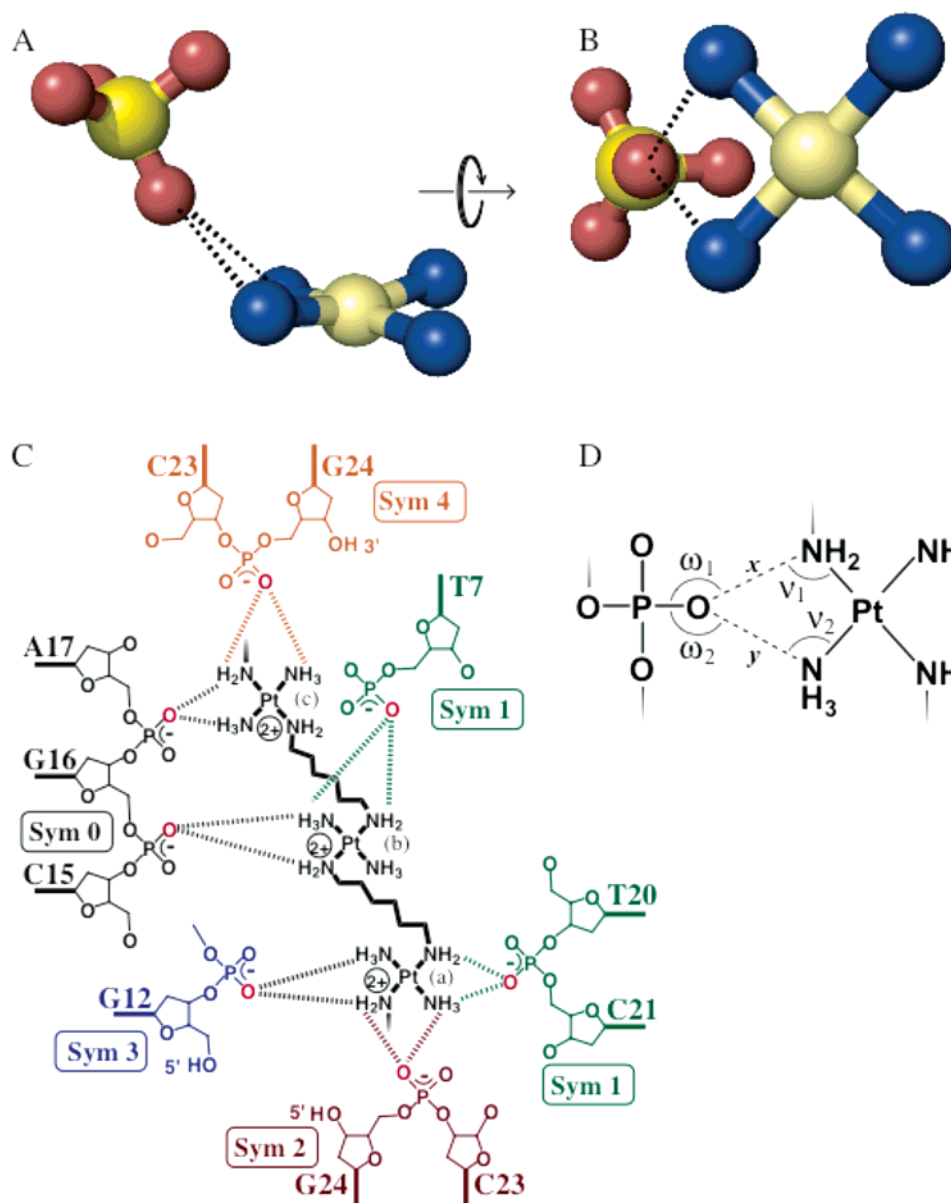


Figure 7. Phosphate Clamps. (A) Phosphate Clamp formed by Pt(II) center (c) and the O2P of A(17). A single phosphate oxygen atom accepts two hydrogens (not indicated) in hydrogen bonds from am(m)ine groups. Oxygen atoms are red spheres, nitrogen atoms are blue, the phosphorus atom is yellow, and the Pt(II) is pale yellow. Hydrogen bonds are dashed lines. (B) Same clamp as in (A) rotated by 90°. (C) Schematic representation of the seven Phosphate Clamps of TriplatinNC^a and the DDD. The dangling amines of TriplatinNC^a are omitted for clarity. (D) Schematic representation of a phosphate clamp illustrating the geometric parameters used to characterize Phosphate Clamps. The parameters of each Phosphate Clamp, with the means and confidence limits, are given in Table 2. The symmetry elements are the same as in Figure 3.

Table 2. Phosphate Clamps: Hydrogen Bonding Distances (Å) and Angles (deg) Involving Ammine/Amine Groups of TriplatinNC and Phosphate Oxygen Atoms (Defined in Figure 6D)

clamp #	Pt atom	atom (residue)	ν_1 (deg)	ν_2 (deg)	ω_1 (deg)	ω_2 (deg)	x (Å)	y (Å)
1	Pt(a)	O2P (C21 ^a)	105	107	113	128	2.88	2.84
2		O2P (G24 ^b)	101	101	129	133	2.84	2.84
3		O2P (G12 ^c)	101	98	115	140	2.93	3.06
4	Pt(b)	O2P (G16)	104	96	115	150	2.98	3.22
5		O2P (T7 ^d)	106	109	139	132	2.93	2.83
6	Pt(c)	O2P (A17)	101	98	144	146	2.96	3.05
7		O1P (G24 ^d)	102	88	145	140	2.75	3.22
8	Pt(d)	O2P (G4)	99	99	115	151	2.94	2.92
	mean		103	100	127	140	2.90	2.95
	($\alpha = 0.05$) ^e		(1.7)	(4.5)	(9.7)	(6.1)	(0.05)	(0.11)

^a Sym 1. ^b Sym 2. ^c Sym 3. ^d Sym 4. ^e 95% confidence limits.

of G(22) is clearly indicated by the close proximity (O6–Na⁺ distance = 2.4 Å, Table 3). In general, determination of Na⁺

positions by X-ray diffraction of macromolecules is problematic because of mixed occupancy of Na⁺ with water molecules,

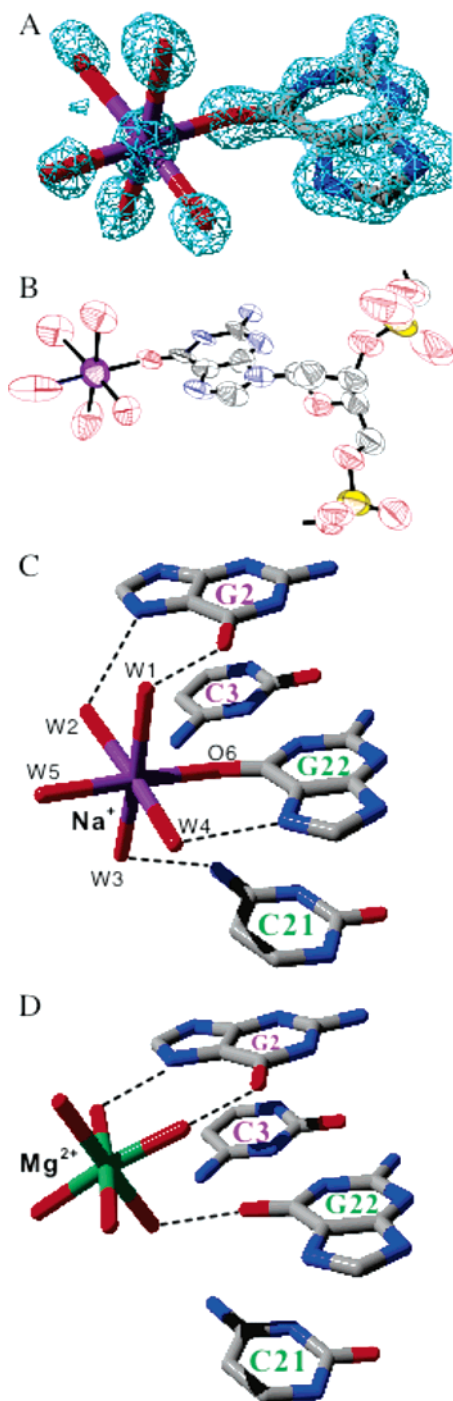


Figure 8. Innershell coordination of a penta-hydrated Na^+ to the O6 atom of a guanine. (A) Electron density map of the Na^+ ion, the guanine to which it is bound, and the first hydration shell, contoured at 1.5σ . (B) ORTEP⁶⁰ diagram indicating 30% of probability. (C) Interactions of the Na^+ ion and its first hydration shells, adjacent to the C(3)–G(22) base pair of the DDD. (D) For comparison, the interactions of Mg^{2+} and its first hydration shell, with the same base pair. Atoms are coded by color.

similar scattering behavior of Na^+ and water, and positional disorder in the solvent region.³⁷ However, there are several structures with sodium ions with reasonable geometry,^{38–41}

Table 3. Bond Distances (Å) and Angles (deg) of $\text{Na}^+(\text{H}_2\text{O})_5\text{O6}(\text{G22})$ Complex

bond	distance (Å)
Na–O1 ^a	2.43
Na–O2	2.46
Na–O3	2.55
Na–O4	2.34
Na–O5	2.46
Na–O6 ^b	2.41
bond	angle (deg)
O1–Na–O2	78
O1–Na–O3	171
O1–Na–O4	93
O1–Na–O5	91
O1–Na–O6	93
O2–Na–O3	93
O2–Na–O4	167
O2–Na–O5	80
O2–Na–O6	98
O3–Na–O4	96
O3–Na–O5	91
O3–Na–O6	85
O4–Na–O5	91
O4–Na–O6	92
O5–Na–O6	176

^a O1, O2... represent the oxygen atoms of the Na^+ first shell water molecules 1, 2... ^b O6 is the O6 atom of G(22).

reviewed by Williams and co-workers.¹⁰ Rich and co-workers observed a Na^+ in the minor groove, directly coordinating two uridine O2 atoms of a dinucleotide.⁴⁰ The position of the Na^+ determined here is consistent with the results of Tl^+ substitution experiments.⁴²

The occupancy of the Na^+ ion observed here is sufficiently close to 100%, and the position is sufficiently localized, that the Na^+ assignment is unambiguous. The assignment is based on coordination geometry, specifically distances within the coordination sphere. The Na^+ electron density peak is well-defined, and is surrounded by a particularly well-ordered octahedron of ligand peaks (Figure 8A). The six Na^+ –O bond lengths are between 2.43 and 2.55 Å (Na^+ –O distances and angles are listed in Table 3). These distances are 0.3–0.4 Å longer than expected for Mg –O distances and 0.3–0.8 Å shorter than expected for $\text{O}\cdots\text{O}$ (water \cdots water) distances. Attempts to fit the Na^+ density to either a magnesium ion or a water molecule resulted in clear shifts of atoms out of sum density, and in difference density adjacent to the central atom and to atoms of the coordination sphere. Therefore, the central electron density peak of the octahedron unambiguously arises from a well-ordered, highly occupied Na^+ .

In the structure described here, the coordination octahedron of the Na^+ is surprisingly regular and well-formed. The standard deviation of the twelve internal angles (which use the Na^+ ion as an apex) is only 6°, with a mean value of 90°. These angles were not restrained during refinement. The regularity of the Na^+ coordination sphere is observable in the electron density maps (Figure 8A). The thermal ellipsoids of the Na^+ ion and its coordination sphere are well-behaved (Figure 8B). The regularity of the octahedron is surprising because Na^+ coordination is not

(37) McFail-Isom, L.; Sines, C.; Williams, L. D. *Curr. Op. Struct. Biol.* **1999**, *9*, 298–304.
 (38) Frederick, C. A.; Williams, L. D.; Ughetto, G.; van der Marel, G. A.; van Boom, J. H.; Rich, A.; Wang, A. H.-J. *Biochemistry* **1990**, *29*, 2538–49.
 (39) Wang, A. H.; Ughetto, G.; Quigley, G. J.; Rich, A. *Biochemistry* **1987**, *26*, 1152–63.

(40) Rosenberg, J. M.; Seeman, N. C.; Kim, J. J. P.; Suddath, F. L.; Nicholas, H. B.; Rich, A. *Nature* **1973**, *243*, 150–4.
 (41) Coll, M.; Solans, X.; Font-Altaba, M.; Subirana, J. A. *J. Biomol. Struct. Dyn.* **1987**, *4*, 797–811.
 (42) Howerton, S. B.; Sines, C. C.; VanDerveer, D.; Williams, L. D. *Biochemistry* **2001**, *40*, 10023–31.

Table 4. Backbone Torsion Angles (α - ζ), Glycosyl Angles (χ), Pseudorotation Phase Angles and Amplitudes, and Sugar Puckers^a

residue	χ (deg)	γ (deg)	δ (deg)	ϵ (deg)	ζ (deg)	α (deg)	β (deg)	phase (deg)	amplitude	pucker
C(1)	-108	-73	153	-147	-161	-68	147	164 (+1) ^b	35	C2'-endo
G(2)	-146	54	87	-163	-66	-57	167	2 (-159)	47	C3'-endo
C(3)	-128	55	98	-173	-75	-69	174	18 (-47)	24	C3'-endo
G(4)	-96	55	137	178	-94	-53	-169	159 (+2)	26	C2'-endo
A(5)	-110	19	129	-173	-95	-42	167	166 (+8)	45	C2'-endo
A(6)	-118	41	135	-169	-99	-60	173	129 (-24)	35	C1'-exo
T(7)	-126	45	110	167	-90	-59	-179	102 (-24)	51	O1'-endo
T(8)	-113	50	129	166	-91	-68	175	119 (-8)	31	C1'-exo
C(9)	-116	60	135	-157	-89	-70	171	143 (-15)	22	C1'-exo
G(10)	-91	48	146	-101	160	-80	166	144 (-3)	42	C1'-exo
C(11)	-99	43	135	-173	-93	-59	167	186 (+22)	27	C3'-exo
G(12)	-114	44	103					83 (-124)	46	O1'-endo
G(24)	-138	49	71					38 (+24)	42	C4'-exo
C(23)	-111	37	126	-176	-81	-68	169	143 (+125)	28	C1'-exo
G(22)	-94	47	141	-127	166	-58	152	132 (-20)	48	C1'-exo
C(21)	-111	56	120	-169	-74	-75	169	137 (+43)	28	C1'-exo
T(20)	-121	61	105	176	-91	-62	-178	122 (-30)	32	C1'-exo
T(19)	-120	72	108	-175	-91	-61	174	149 (+5)	40	C2'-endo
A(18)	-114	58	117	162	-83	-62	168	114 (-14)	34	C1'-exo
A(17)	-107	48	149	180	-98	-69	177	159 (-14)	26	C2'-endo
G(16)	-96	50	146	163	-87	-65	-165	184 (+15)	39	C3'-exo
C(15)	-137	67	82	-168	-77	-59	-179	17 (-25)	39	C3'-endo
G(14)	-98	45	115	173	-101	-62	156	119 (-11)	37	C1'-exo
C(13)	-137	44	151	-135	-90	-84	167	108 (-56)	24	C1'-exo

^a Backbone torsion angles are O3'-P- α -O5'- β -C5'- γ -C4'- δ -C3'- ϵ -O3'- ζ -P-O5'.⁶¹ ^b Deviation from the control DDD.

generally confined to a well-ordered octahedron.³¹ By comparison, a hexa-coordinated sodium ion identified in the minor groove of (ApU)₂ by Rich and co-workers,⁴⁰ which makes direct base contacts in the minor groove (to two O2 atoms of uridine residues), shows a standard deviation of the twelve internal angles of 12°, with a mean value of 91°. In that structure, the longest Na⁺-O distance is 2.9 Å, well beyond the optimum.

The water molecules in the Na⁺ first shell form multiple hydrogen bonds to the DNA. These hydrogen bonds are to the guanine O6 and N7 positions of G(2) and to the N7 position of G(22) (in each the water molecule donates a hydrogen atom, Figures 3 and 8C). In addition one of the Na⁺ first shell water molecules forms a hydrogen bond with the exocyclic N4 amino group of cytosine of C(21) (this water *may be* acting as a hydrogen bond acceptor). The first Na⁺ hydration shell does not engage in hydrogen-bonding interactions with symmetry-related duplexes, and so does not appear to be an artifact of lattice interactions.

In previous high-resolution X-ray structures of unliganded forms of the DDD, a fully hydrated magnesium ion (Mg²⁺-(H₂O)₆) is generally located in the major-groove, adjacent to the G(2)-C(23) and C(3)-G(22) base pairs.^{28,34,43} The first hydration shell of this Mg²⁺ ion interacts with the O6 and N7 positions of guanine residues (Figure 8D) and with phosphate oxygens of an adjacent duplex. This major groove magnesium is effectively replaced by a Na⁺ ion in the DDD-TriplatinNC complex. In contrast to the Na⁺ ion, the first shell hydration layer of Mg²⁺ in bld084 does form lattice contacts, interacting with phosphate oxygens of adjacent duplexes in the crystal.

DNA Conformation. In solution, noncovalent polynuclear Pt(II) complexes with high cationic charge are found to stabilize various DNA conformational states, such as B, A, and Z conformation.^{7,8} The DNA in the DDD-TriplatinNC complex described here is in the B-conformation. To infer the effects of TriplatinNC binding on DNA conformation, we compare it with

other high-resolution DDD structures, in particular structure bdl084,²⁸ which is the highest resolution, nonmodified DDD structure determined thus far. Phosphodiester backbone torsion angles, glycosyl angles, and sugar puckers are given in Table 4. Helical parameters are shown in Figures 1S and 2S; minor- and major-groove widths are shown in Figure 3S (see Supporting Information).

The Backbone: Sugar Puckers. We anticipate that at the high resolution of this structure, sugar puckering is not significantly affected by restraints. Sixteen of 24 sugar puckers of the DDD-TriplatinNC complex are significantly different from those in the control DDD (Table 4). The sugar puckers of residues G(2) and C(23) show the largest differences in the DDD-TriplatinNC complex from in the control DDD (bdl084). These differences may arise from differences in direct and first shell water interactions of Na⁺ versus Mg²⁺ (Figure 8). More modest differences observed at G(12) and C(13) may arise from interactions of TriplatinNC^b, which bridges between two symmetry-related DNA duplexes. TriplatinNC^a interacts with many of the phosphate oxygens of residues C(13) through A(18), which pair with T(7) through G(12). These sugar puckers are generally the same in the TriplatinNC-DNA complex and the control DNA.

Helical Parameters. TriplatinNC^a forms total twenty hydrogen bonds with DNA phosphate oxygens and only two hydrogen bonds with base atoms. Those two hydrogen bonds involve a single guanine base, at the N7 and O6 positions. Therefore, TriplatinNC^a may alter DNA conformation in this region by direct short-range interactions with DNA bases. TriplatinNC^a-phosphate hydrogen bonds and longer range electrostatic interactions could influence helical parameters. TriplatinNC^b forms hydrogen bonds with the O6 of G(12) as does the pentahydrated sodium, which coordinates the O6 of G(22). In addition, the first shell water molecules of the Na⁺ ion form

(43) Minasov, G.; Tereshko, V.; Egli, M. *J. Mol. Biol.* **1999**, *291*, 83-99.

hydrogen bonds with the bases in a manner that is distinct from the interactions of the hexa-hydrated magnesium of the control DDD.

The Backbone: BI vs BII. B-DNA conformation is characterized by BI, the most frequent, or BII, depending on the torsion angles ϵ and ξ .^{44,45} These torsion angles influence the positions of phosphate groups and modulate the width of the minor groove. The difference in the torsion angles ϵ and ξ is commonly used to characterize the BI/BII status. $\epsilon - \xi$ of roughly -90° indicates BI and roughly $+90^\circ$ indicates BII. The DDD-TriplatinNC complex is wholly in the BI conformation, with $\epsilon - \xi$ in the range of -160 to $+20$.

Inter-Base and Inter-Base Pair Parameters. Throughout the duplex, significant deviations from the control DDD are observed in many parameters. In some of the parameters, such as shear, stagger, buckle, and propeller twist,⁴⁶ the largest deviations are observed in the G-tracts, possibly because of direct interaction of Na^+ and TriplatinNC^b with the DNA bases. A common feature of both base-base (Figure 1S) and inter-base pair (Figure 2S) parameters is that many of the greatest deviations from the control DDD are found where a Mg^{2+} ion in the control DDD is replaced by a Na^+ ion here. These differences are especially apparent for the interbase pair parameters such as shift, roll, and rise (Figure 2S). Electrostatic forces, arising from localization of charge directly adjacent to the DNA, and/or hydrogen bonding interactions appear to pull neighboring bases into hydration layer of the sodium. As described above, water ligands of the Na^+ coordination sphere form an extensive hydrogen bonding network in the major groove.

Global Conformation and Groove Width. There are significant differences in the minor-and major groove widths of the DDD-TriplatinNC complex and the control DDD (Figure 3S). The minor-groove of the DDD-TriplatinNC complex is wider at the T(7)-A(18) base pair than the control DDD. This change in conformation may be related to electrostatic interactions of phosphate groups with TriplatinNC^a. Two opposing (across the minor groove) phosphate groups interact with two different cationic centers of TriplatinNC^a (Figure 5). The positions of the two cationic centers are such that the minor groove appears to be pulled open by the two cationic centers.

This effect differs from that described previously for Mg^{2+} . Groove narrowing was attributed to the interaction of opposing phosphate groups with a *single* cationic center.³⁴ The minor groove of both the control DDD and the DDD-TriplatinNC complex lack such a Mg^{2+} in the lip of the groove, and do not display acute groove narrowing. For the major groove width the deviation of the DDD-TriplatinNC complex from bdl084 may be associated with the sodium ion in the major groove.

In the program Curves 5.3,³³ the parameter UU is a measure of axial bending, giving the angle formed by the axis segments of the terminal sections of the DNA duplex. $\text{UU} = 28^\circ$ for the DDD-TriplatinNC complex. However, another parameter, PP, is the angle between the vectors formed the two axis reference

points at either end of the fragment. $\text{PP} = 39^\circ$ for the DDD-TriplatinNC complex. Ordinarily the UU and PP are within a few degrees. Differences in UU and PP ($\text{UU} \gg \text{PP}$) help to signal if a significant part of the UU angle comes from a deformation of the ends of the fragment analyzed, rather than from internal bending or kinking.⁴⁷ At any rate, the axial bend and the axial path length shortening ratio are greater in the DDD-TriplatinNC complex ($\text{UU} = 28^\circ/2.4\%$) than in the control DDD ($\text{UU} = 12^\circ/0.66\%$). This difference is apparent in Figure 9, which shows a superimposition of the two structures.

Discussion

Backbone Tracking and Groove Spanning: Novel Modes of DNA Binding. Previously described DNA ligands can be broadly broken down into intercalators^{1,2} and groove binders,³ and as reviewed by Wilson.⁴ The DNA ligand described here, TriplatinNC does not intercalate nor does it bind in either groove. It binds to phosphate oxygen atoms and thus associates with the backbone. TriplatinNC presents an unexplored mode of nucleic acid binding with the potential for wide applicability. TriplatinNC also illustrates the utility of modular binding elements, such as the tetra-am(m)ine Pt(II) coordination unit, for design (or selection) of nucleic acid ligands.

Oxygen Selectivity. TriplatinNC contains multivalent cationic centers, and planar arrays of directional hydrogen bond donors, linked by flexible hydrophobic segments. In binding to DNA, TriplatinNC shows selectivity *for* phosphate oxygens, and *against* other oxygen atoms and particularly *against* nitrogen atoms. The selectivity of TriplatinNC extends to O2P over O1P, at least in B-form DNA. To our knowledge TriplatinNC is the first phosphate-selective DNA ligand characterized thus far. Preferential interaction with phosphate oxygens causes TriplatinNC^a to track the backbone (Figure 4), linking adjacent phosphate groups, and to span the minor groove (Figure 5).

The Phosphate Clamp. The tetra-am(m)ine Pt(II) coordination unit forms a bidentate complex with a single OP atom, a structure that we call a Phosphate Clamp. A Phosphate Clamp is a cyclic structure in which a single OP accepts two hydrogen bonds, one each from two am(m)ine ligands of a single Pt(II) center. The geometry and type of oxygen atom are highly conserved in the eight Phosphate Clamps observed in the DDD-TriplatinNC complex. The geometric parameters used to characterize Phosphate Clamps are given in Figure 7D. Values for each clamp and the mean values are given Table 2. Each tetra-am(m)ine square-planar Pt(II) coordination unit has the potential to form four Phosphate Clamps. A Phosphate Clamp requires *cis*-am(m)ine ligands of Pt(II). Mutually *trans*-am(m)ine ligands do not form Phosphate Clamp because the proton donors are too far apart and in opposing directions.

A Phosphate Clamp is a small modular nucleic acid binding unit, with specific and conserved geometry. In the present structure, the four observed Pt(II) centers of TriplatinNC^a and TriplatinNC^b contain a total of 16 potential Phosphate Clamps. The eight Phosphate Clamps observed here involve eight OPs. Each Pt(II) center engages in at least one Phosphate Clamp (Figures 3 and 7C).

The high frequency of occurrence of this cyclic motif, along with conservation of its geometry, suggests favorable stability. One could in principle take advantage of the modularity,

(44) Prive, G. G.; Heinemann, U.; Chandrasegaran, S. K.; S., L.; Kopka, M. L.; Dickerson, R. E. *Science* **1987**, *238*, 498–504.

(45) Hartmann, B.; Piazzola, D.; Lavery, R. *Nucleic Acids Res.* **1993**, *21*, 561–8.

(46) Dickerson, R. E.; Bansal, M.; Calladine, C. R.; Diekmann, S.; Hunter, W. N.; Kennard, O.; Lavery, R.; Nelson, H. C. M.; Olson, W. K.; Saenger, W.; Shakked, Z.; Sklenar, H.; Soumpasis, D. M.; Tung, C.-S.; von Kitzing, E.; Wang, A. H.-J.; Zhurkin, V. B. *J. Mol. Biol.* **1989**, *205*, 787–91.

(47) Lavery, R. Personal communication, 2006.

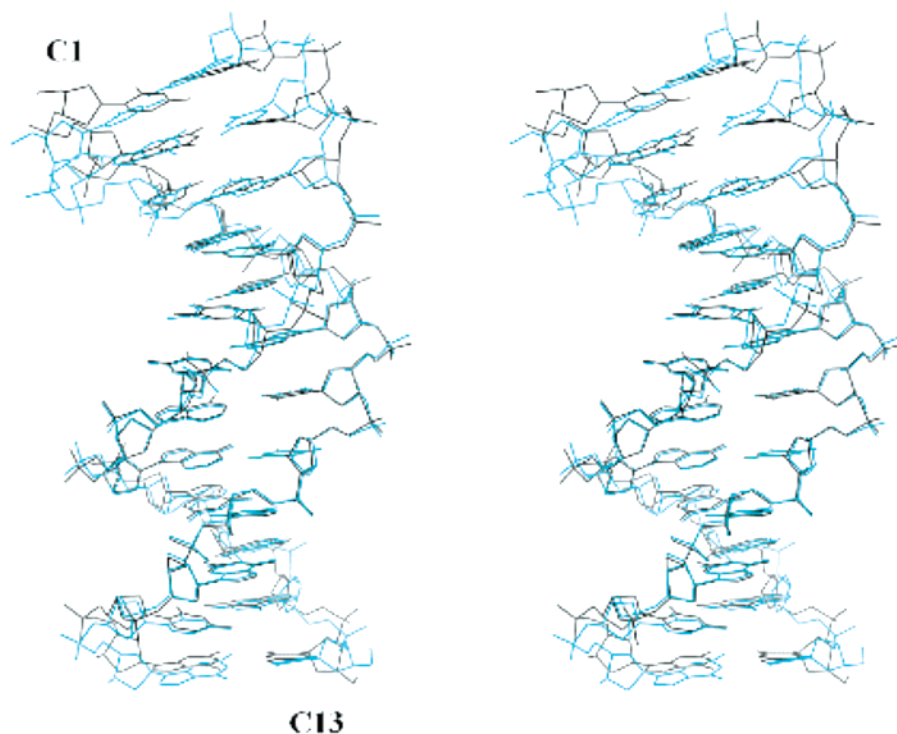


Figure 9. Stereo superimposition of the DDD–TriplatinNC complex (cyan) onto the control DDD (black). The superimposition was performed using residues A(6)–T(19), A(7)–T(18), and T(8)–A(17). The residues of these three continuous base pairs gave a smaller RMS deviation of atomic positions than any other set of three continuous base pairs.

predictability, and stability to assemble Phosphate Clamps in virtually any given three-dimensional arrangement. Tetra-am(m)ine Pt(II) coordination units could be assembled with specified spatial and geometrical dispositions to bind specifically to various nucleic acid structures. For example, relatively short linkers would favor binding A-form DNA or RNA, whereas relatively long linkers would favor binding to B-form DNA. More complex and rigid three-dimensional arrangements could be designed (or selected) that bind to ribosomal RNA, G-quartets or other globular nucleic acids. The complex described here may lead to new approaches in drug design.

TriplatinNC, the Super Arginine. We hypothesized that interactions of the small DNA ligand TriplatinNC might mimic those of certain amino acids in nucleic acid–protein complexes. Indeed the interactions of the am(m)ines of TriplatinNC are similar in some ways to those of the guanidino group of arginine. We have examined interactions of all 336 arginines within the large ribosomal subunit of *Haloarcula marismortui*. A crystal structure of the HM LSU (1JJ2) was determined to 2.4 Å resolution by Steitz and Moore.^{48,49} The atomic positions of the vast majority of HM LSU (1JJ2) are well-characterized (2.4 Å resolution), and, as of this writing, are more accurately determined than any nucleic acid complex of equivalent size. The results show that arginine, like TriplatinNC is selective for phosphate oxygens. The guanidino groups of the 336 arginine residues in the proteins associated with the HM LSU form 277 hydrogen bonds with OP atoms and only 35 hydrogen bonds to base oxygen atoms and 19 hydrogen bonds to base nitrogen atoms (base-pair specific H-bonding by amino acids is described in ref 50). Arginine shows a phosphate clamping ability that is

analogous to TriplatinNC, although significantly attenuated. Sixty-nine clamp-like structures are observed in the HM LSU, in which a single OP accepts two hydrogen bonds from a single arginine guanidino group. The HM LSU contains several binary complexes in which a single arginine guanidino group forms clamp-like structures with two OP atoms. This motif was described previously as an Arginine Fork.⁵¹ A single arginine is limited to two clamps, and forms such binary complexes with low frequency, at least in the HM LSU. TriplatinNC can form four clamps and forms binary and higher order complexes (Figure 6) with high frequency in the DNA complex described here.

Timsit and Moras⁵² previously suggested that dCG steps in supramolecular assemblies of DNA can anchor adjacent duplexes. The amino groups of cytosines form hydrogen bonds to OP atoms in a mode of interaction that is reminiscent of the phosphate clamp with the distinction that a given dCG step appears to associate with several OP atoms rather than a single OP atom, as in a phosphate clamp.

DNA Distortion. Mirzabekov, Rich and Manning^{53,54} suggested that charge neutralization of phosphate groups might drive DNA distortion and bending. They proposed that asymmetric charge neutralization by cationic protein side chains, could lead to “phosphate collapse”. That model was extended by Rouzina and Bloomfield,⁵⁵ who proposed that mobile cations such as Mg²⁺ can contribute electrostatically to DNA bending.

(48) Ban, N.; Nissen, P.; Hansen, J.; Moore, P. B.; Steitz, T. A. *Science* **2000**, *289*, 905–20.

(49) Klein, D. J.; Schmeing, T. M.; Moore, P. B.; Steitz, T. A. *EMBO J.* **2001**, *20*, 4214–21.

(50) Seeman, N. C.; Rosenberg, J. M.; Rich, A. *Proc. Natl. Acad. Sci. U.S.A.* **1976**, *73*, 804–8.

(51) Calnan, B. J.; Tidor, B.; Biancalana, S.; Hudson, D.; Frankel, A. D. *Science* **1991**, *252*, 1167–71.

(52) Timsit, Y.; Moras, D. *EMBO J.* **1994**, *13*, 2737–46.

(53) Manning, G. S.; Ebralidse, K. K.; Mirzabekov, A. D.; Rich, A. *J. Biomol. Struct. Dyn.* **1989**, *6*, 877–89.

(54) Mirzabekov, A. D.; Rich, A. *Proc. Natl. Acad. Sci. U.S.A.* **1979**, *76*, 1118–21.

(55) Rouzina, I.; Bloomfield, V. A. *Biophys. J.* **1998**, *74*, 3152–64.

In the Rouzina and Bloomfield model, a divalent cation can repel and displace other counterions, leading to strong attraction with proximal phosphate groups. The result is DNA bending by electrostatic collapse around a divalent cation. Monovalent cations, when partially dehydrated as in the DDD–TriplatinNC complex, may also facilitate DNA bending.

We observe that the DNA conformation in the DDD–TriplatinNC complex differs somewhat from that of the native DDD structure (NDB entry bdl084). In comparison with the control structure, the axial bend is greater in the DDD–TriplatinNC complex, helical parameters are perturbed and the minor groove width profile is modestly impacted. The locus of the distortion suggests it does not arise, at least directly, from the highly charged TriplatinNC molecule that extends along the DNA backbone (TriplatinNC^a), or the more disordered TriplatinNC molecule (TriplatinNC^b).

The substitution of a fully hydrated Mg²⁺ in the native DDD for a partially dehydrated Na⁺ ion, located directly on the floor of the major groove (interacting with O6 of a G), may contribute to DNA deformation. In previous high-resolution DDD structures, a hexa-hydrated Mg²⁺ ion is located within the major-groove at one of the G-tracts. This ion is located at the nexus of an axial bend.^{28,34} First-shell water molecules of the Mg²⁺ ion form hydrogen bonds to DNA bases, particularly to guanines. The DNA complex with TriplatinNC lacks observable Mg²⁺ ions, even though MgCl₂ was included at a concentration similar to that in the control DDD crystallization solution. The fully hydrated Mg²⁺ ion has been displaced by a partially dehydrated and particularly well-ordered Na⁺ ion. The location of this Na⁺ ion, associated with a guanine, in the major groove, was predicted.^{10,42}

It may be that TriplatinNC, which is highly charged, displaces Mg²⁺ by long-range electrostatic competition. An alternative possibility is that the conformation of DNA induced by TriplatinNC favors replacement of fully hydrated Mg²⁺ by penta-hydrated Na⁺. This possibility is supported by the unusually geometric and well-formed octahedron of ligands [five waters plus O6(G)] surrounding the Na⁺. The five first shell waters interact simultaneously both with DNA and with the Na⁺. The Na⁺–ligand geometry seems nearly ideal and is not perturbed by direct proximity of the floor of the major groove. Thus the DNA deformation appears to present a favorable binding pocket for penta-hydrated Na⁺. Alternatively it can be said that the hydrated, deformed DNA presents a well-formed binding pocket for naked Na⁺.

In the control DDD, a partially disordered spermine molecule is observed in the major groove of the unbent G-tract, which lacks a Mg²⁺ ion. The DDD–TriplatinNC complex lacks spermine molecules; spermine was not contained in the crystallization solution. The lack of significant differences between DDD–TriplatinNC and the control DDD in this region suggests that spermine in the major groove of a G-tract does not contribute significantly to conformational distortion.

Biological Relevance. This contribution has defined new backbone-binding modes of binding to DNA, termed Backbone-Tracking and Groove Spanning. Both modes involve arrays of Phosphate Clamps.

Preassociation with DNA may be important in efficiency and specificity of covalent cross-linking.²⁰ The Pt(II) centers of BBR3464 (Figure 1C) could transiently engage in Phosphate Clamps in preassociated complexes, prior to covalent modification of the DNA.

Although the formal charge is +8, TriplatinNC displays micromolar activity against a human ovarian cancer cell line⁵⁶ and is thus the first example of a noncovalent platinum compound with cytotoxicity equivalent to cisplatin. TriplatinNC displays *in vivo* antitumor activity in 2008 ovarian carcinoma xenografts (Farrell, unpublished). Accordingly, the noncovalent interactions of polynuclear platinum complexes may play significant roles in inhibiting the growth of cancer cells. Cisplatin's major DNA adduct, 1,2-intrastrand cross-link, severely distorts DNA. The distortion recruits high mobility group (HMG) and other proteins which may shield the covalent cisplatin-DNA lesion from DNA repair.^{13,57} The DNA distortions induced by the noncovalent interactions of TriplatinNC may also be responsible for protein recruitment, although the distortions are modest in comparison to those of cisplatin.

Another feature of TriplatinNC is that the cellular uptake is significantly enhanced over the “parent” BBR3464.⁵⁶ Studies on mast cells appear to show selective uptake of TriplatinNC into tumor cells compared to normal mast cells.⁵⁸ The higher positive charge a polynuclear Pt(II) species possesses, the more cellular uptake is observed. It is interesting to speculate that, for cytotoxicity, the relatively weak noncovalent interactions of TriplatinNC in comparison to the covalent binding of cisplatin are offset by the very high cellular uptake. This feature and high DNA affinity of TriplatinNC may help a biologically relevant component access to DNA in a tumor cell. Thus TriplatinNC could also be a carrier device for drugs or genes.⁵⁹ Accordingly, the results presented here support further studies aimed at a structure–function–activity relationship for noncovalent compounds of this type.

Acknowledgment. This research was supported by National Institutes of Health RO1CA78754 to N.F. and by the Japan Society for the Promotion of Science to S.K. We thank Chiaolong Hsiao and Drs. Nick Hud, Akira Odani, Yun Qu, and Hirofumi Ohishi for helpful discussions and Dr. Alex Hegmans for the synthesis of the Pt(II) compound. Atomic coordinates and structure factors have been deposited in the NDB (entry code DD0086) and PDB (entry code 2DYW).

Supporting Information Available: DNA conformational parameters. This material is available free of charge via the Internet at <http://pubs.acs.org>.

JA062851Y

- (56) Harris, A. L.; Yang, X.; Hegmans, A.; Povirk, L.; Ryan, J. J.; Kelland, L.; Farrell, N. P. *Inorg Chem.* **2005**, *44*, 9598–600.
- (57) Ohndorf, U. M.; Rould, M. A.; He, Q.; Pabo, C. O.; Lippard, S. J. *Nature* **1999**, *399*, 708–12.
- (58) Harris, A. L.; Ryan, J. J.; Farrell, N. *Mol. Pharmacol.* **2006**, *69*, 666–72.
- (59) Farrell, N.; Kloster, M. G. B., US Patent 6,310,047.
- (60) Johnson, C. K. *Ortep II*; Oak Ridge National Laboratory, Report Rnl-5138; Oak Ridge, Tennessee, 1976.
- (61) Saenger, W. *Principles of Nucleic Acid Structure*; Springer-Verlag: New York, 1984.